

## **ANCHOR PULL-OUT TESTS - INFLUENCE OF BOUNDARY CONDITIONS AND MATERIAL PROPERTIES**

V. Slowik, A.M. Alvaredo and F.H. Wittmann,  
Laboratory for Building Materials, Swiss Federal Institute of Technology  
Zurich, Switzerland

### **Abstract**

Following an invitation from RILEM to participate in a Round Robin, anchor pull-out tests were run. In addition to specimen size and boundary conditions, the material properties were varied. Specimens made of structural concrete, mortar and lightweight concrete were tested. It was shown that the cracks in the specimens propagate predominantly in a crack opening mode rather than in a crack sliding mode. The final crack patterns were significantly influenced by the boundary conditions but proved to be independent of the material used.

### **1 Introduction**

In 1990, RILEM issued an invitation for a Round Robin test and analysis on the fracture of the anchorage of bolts in concrete (RILEM, 1990). During the following years several researchers have run the corresponding experiments and numerical simulations.

The experimental results presented here were obtained under the conditions outlined in RILEM (1990). However, in addition to specimen

size and boundary conditions, the material properties were varied. The intention was to investigate the influence of the meso-level characteristics of the material on the fracture process, especially on the crack pattern.

In a first part of the experimental program (series S1..S3) the distance between the supports was varied following the guidelines for this Round Robin test. The second part (series M1..M3) contained tests with different cementitious materials. Structural concrete, mortar and lightweight concrete were used. The objective of the third part (series R1..R3) was to investigate the influence of the lateral restraint. In these series different cementitious materials were also used.

In the interpretation of the test results special attention was given to the observed crack pattern.

## 2 Experiments

### 2.1 Specimen preparation

The tested concrete plates had the dimensions  $6d \times 6d \times 100$  mm, with  $d=150$  mm for series S1..S3 and M1..M3, and  $d=50$  mm for series R1..R3, see Fig. 1. The lateral deformation of the specimens was not restrained for series S1..S3 and M1..M3 ( $K=0$  in Fig. 1) whereas it was restrained for most of the specimens belonging to series R1..R3 ( $K=\infty$ ). In the series S1, S2 and S3, the distance  $a$  between the lateral edge of the anchor bolt and the supports was varied, as indicated in Table 1.

Table 1. Number of specimens, specimen dimensions and material types for the test series

Series	number of specimens	$d$ [mm]	$a$ [mm]	material	$K$
S1	3	150	$2d=300$	A	0
S2	3	150	$d=150$	A	0
S3	3	150	$d/2=75$	A	0
M1	3	150	$2d=300$	A	0
M2	3	150	$2d=300^*$	B	0
M3	2	150	$2d=300$	C	0
R1	2	50	$2d=100$	A	$\infty^{***}$
R2	3	50	$2d=100^{**}$	B	$\infty^{***}$
R3	3	50	$2d=100$	C	$\infty^{****}$

\* One specimen in this series was tested with  $a=75$  mm.

\*\* One specimen in this series was tested with  $a=62.5$  mm.

\*\*\* One specimen in this series was tested with  $K=0$ .

\*\*\*\* One specimen in this series was tested with  $K=0$  and one specimen with  $0 < K < \infty$ .

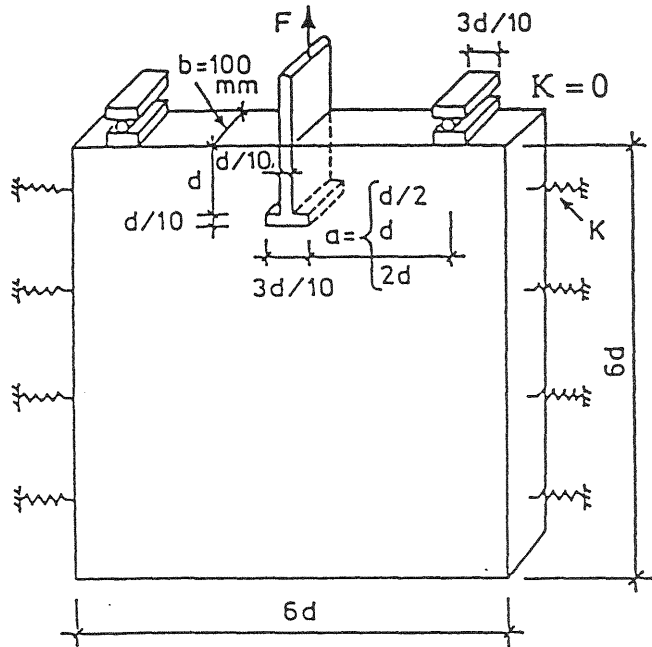


Fig. 1. Specimen geometry (RILEM, 1990)

Table 2. Material characteristics

Material	A structural concrete	B mortar	C lightweight concrete
Max. grain size [mm]	16	4	10 (expanded clay)
Cement content [kg/m <sup>3</sup> ]	350	410	4500
Water content [kg/m <sup>3</sup> ]	175	205	200
Aggregate content [kg/m <sup>3</sup> ]	1890	1790	1000 l/m <sup>3</sup> (expanded clay) +400 kg/m <sup>3</sup> (sand)
Compr. strength [MPa]	39.3±4.1*	22.6±0.7**	28.2±2.1**
Mod. of elasticity [MPa]	37600	18290	15070
Fracture energy [N/m]	93.17±10.31***	72.60±5.76***	40.35±3.55***
Density [g/cm <sup>3</sup> ]	2.41	2.20	1.56

\* determined on 150 mm cubes

\*\* determined on 300 mm high cylinders, diameter 150 mm

\*\*\* determined on 200\*200\*80 mm<sup>3</sup> wedge splitting specimens, notch length 107 mm

Table 2 contains the concrete composition and the mechanical properties at the age of testing. In order to avoid friction between the shaft of the anchor bolt and the adhering concrete, the metal was coated, except for the upper surface of the bolt head. A teflon coating was applied to the bolts in the series S1..S3, while for the series M1..M3 and R1..R3 a 0.5 mm thick paraffin layer was used.

The specimens were stored under wet burlap for 2 days and then kept at 20°C and 70% relative humidity until the age of testing. The latter ranged from 27 to 34 days.

## 2.2 Test setup and experimental procedure

An electro-mechanical testing machine with vertical loading direction was used. It must be pointed out that in this loading system the self weight of the specimen acted as an additional load on the anchorage. For some of the specimens the self weight was compensated by applying an upward pressure to the specimen's downside. No influence of the self weight on the crack pattern could be found. For the tests without compensation the peak loads were corrected by adding the self weight.

Fig. 2 shows the device used to restrain the lateral deformation (series R1..R3). The horizontal distance between the specimen boundaries was measured at a line 5 cm below the specimen's upper surface and kept constant during the test by twisting the screws of the four restraining bars. Two 20 mm thick steel plates on both sides of the specimen prevented load concentrations. The strain in the bars was measured.

In the tests, the vertical displacement  $v$  of the head of the anchor bolt relative to a point at the concrete surface 200 mm beneath the anchor bottom was used as control parameter, its rate of application being set equal to 1  $\mu\text{m/s}$ .

## 3 Experimental results

### 3.1 Load-displacement curves

The force  $P$  applied to the supports was recorded as function of the displacement  $v$ . Figs. 3 and 4 show two typical load-displacement curves. The load-displacement curves for the specimens without horizontal displacement restraint exhibit a shape similar to the one shown in Fig. 3. Table 3 contains the mean peak loads  $P_{\text{max}}$  and the mean displacements  $v_m$  at peak load for the different series.

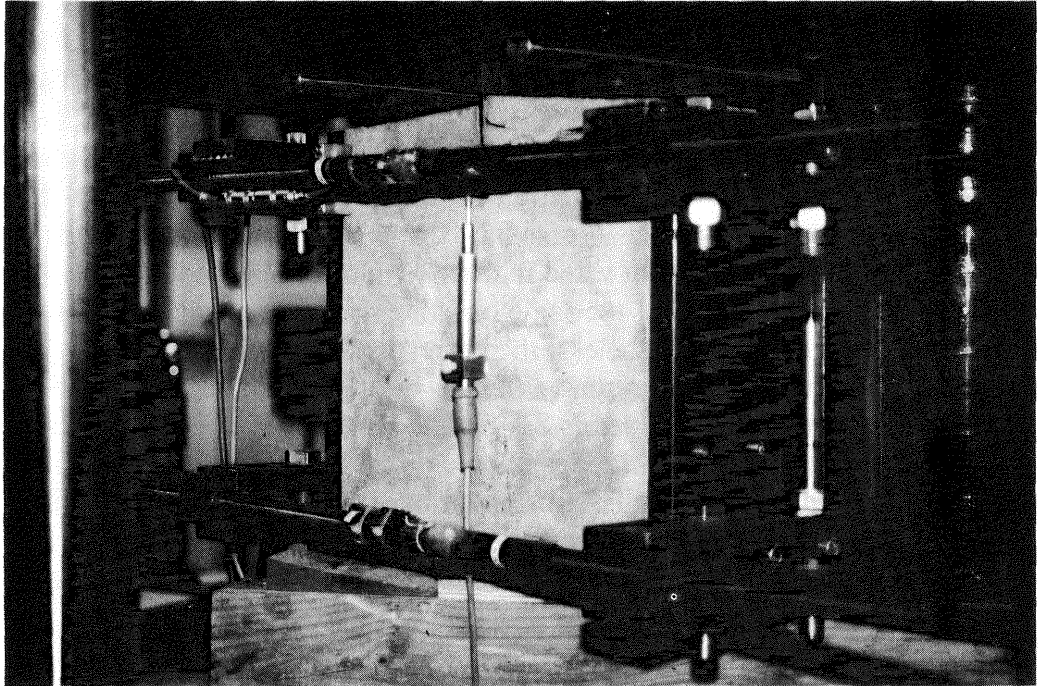


Fig. 2. Device for restraining the horizontal displacement

The load-displacement curves for specimens with horizontal displacement restraint exhibit two peaks, see Fig. 4. The first one has the same value and corresponds to the same displacement  $v$  as for the

Table 3. Peak loads and corresponding displacements

Series	Peak load $P_{\max}$ [kN]	Displacement at peak load $v_m$ [ $\mu\text{m}$ ]
S1	38.4 $\pm$ 1.8	82.7
S2	61.9 $\pm$ 5.2	255.4
S3	117.1 $\pm$ 12.6	248.0
M1	29.4 $\pm$ 2.5	81.6
M2	21.1 $\pm$ 1.3*	95.0
M3	15.4 $\pm$ 0.4	67.5
R1 for $K=0$	18.3	44
for $K=\infty$	25.2	3529
R2 for $K=0$	13.7**	44.3
for $K=\infty$	33.2**	2469
R3 for $K=0$	8.2	64.4
for $K=\infty$	20.8	1306
for $0 < K < \infty$	13.2	3868

\* This mean value was determined only from the specimens with  $a=2d$ .

\*\* These values were determined only from specimens with  $a=2d$ .

specimens without lateral restraint. The second one is higher and the corresponding displacement  $v$  much larger than that at the first peak. This indicates the occurrence of two different failure mechanisms in the fracture process of the specimens with horizontal restraint. The force in the two upper restraining bars amounted to approximately 60 kN. For the unrestrained specimens the horizontal displacement increased nearly linearly with the displacement  $v$  and reached a value of almost 1 mm.

For the series S1 and M1 the same concrete mix and the same specimen geometry were used. Nevertheless, the corresponding peak loads differ by about 20%. The reason for this different behavior might be the teflon coating of the anchor bolt in series S1, S2 and S3 not fully avoiding friction between the bolt shaft and the concrete. Surface irregularities resulted in the applied load being partially transmitted by friction along the shaft. For the series M1, M2 and M3 this effect had no significance because of the relatively thick and yielding paraffin coating. The displacements at peak load were equal for the series S1 and M1.

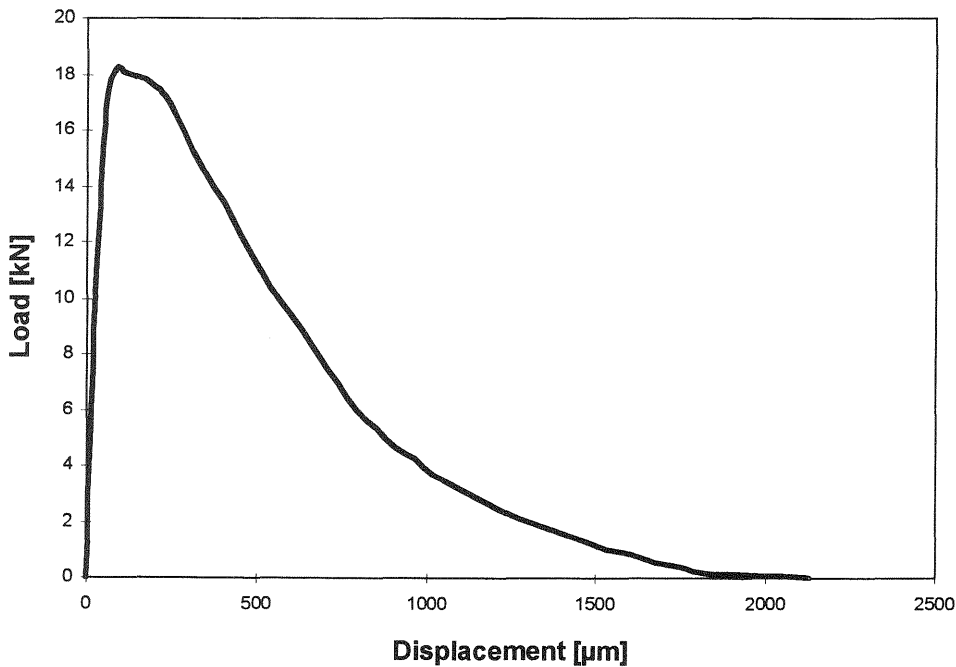


Fig. 3. Load-displacement curve for a specimen of series M2 (without lateral restraint)

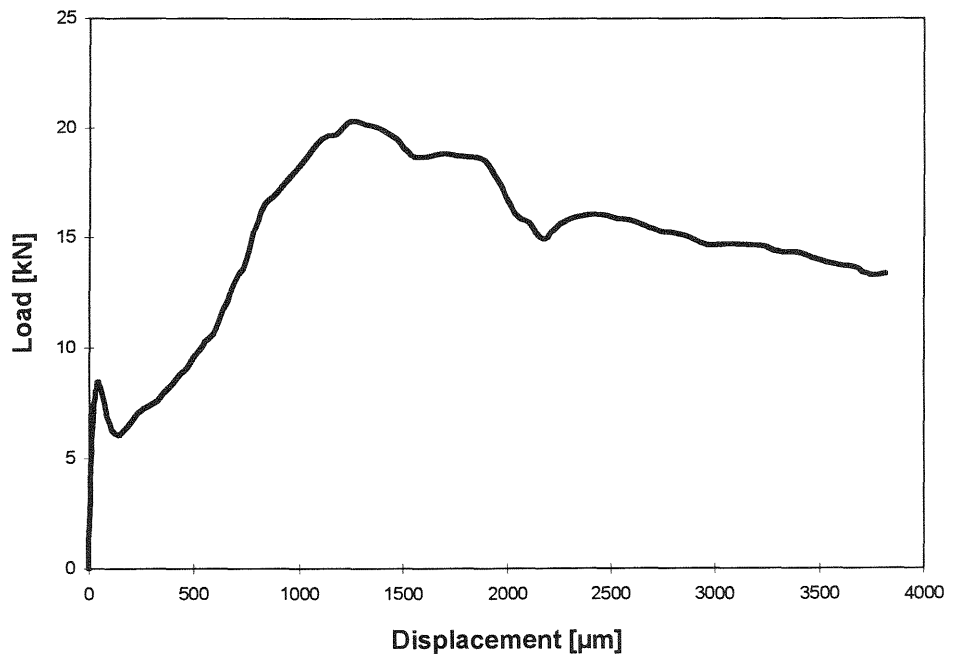


Fig. 4. Load-displacement curve for a specimen of series R3 (with lateral restraint)

It is worth pointing out that the peak load for the series M3 (lightweight concrete) is lower than that for series M2 (mortar) although the compressive strength of the lightweight concrete is higher than that of the mortar. This can be explained by the higher fracture energy of the mortar.

### 3.2 Crack pattern for the non-restrained specimens

From the viewpoint of classical continuum mechanics it should be expected that two triangular prisms be torn apart at failure. Initially, the crack pattern exhibited the expected straight cracks, here called primary cracks, starting at the top side of the anchor head. This crack pattern corresponded to the maximum load. For higher displacements  $v$  either one or two additional cracks were formed splitting the specimen in the vertical direction. These cracks are here called splitting cracks.

The pattern of splitting cracks varied with the boundary conditions. For  $a=d/2$  one vertical splitting crack starting from the bottom of the anchor head was formed, see Fig. 5, whereas for  $a=2d$  two inclined cracks near the specimen boundaries appeared, see Fig. 6. Either crack pattern could be observed for  $a=d$ . In some cases only one of the primary cracks reached the top side of the specimen.

The same qualitative crack patterns were observed for structural concrete, mortar and lightweight concrete. There seems to be no difference in the fracture process for the different materials used here.

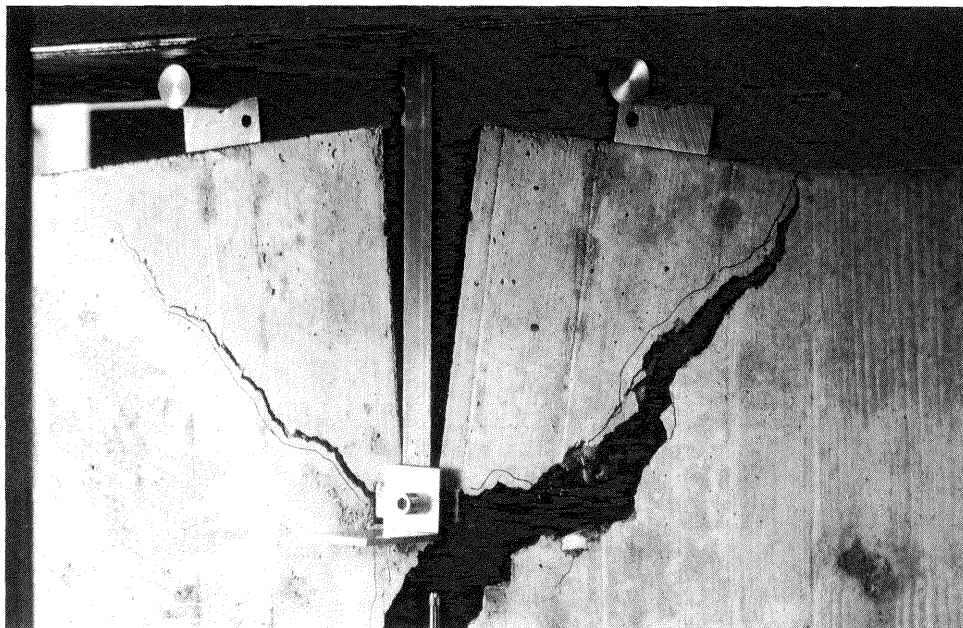


Fig. 5. Specimen S3-1, final crack pattern

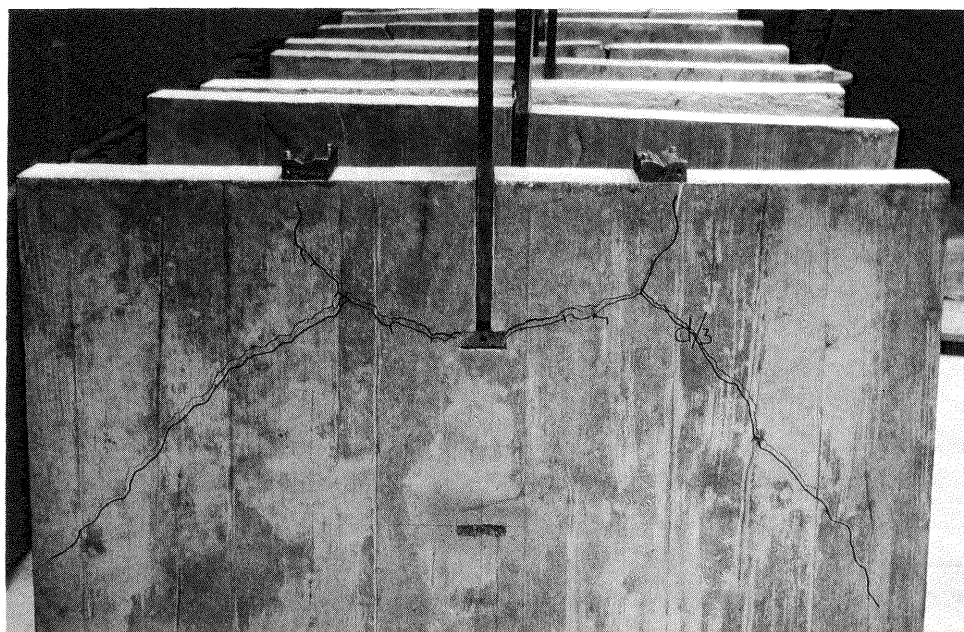


Fig. 6. Specimen S2-3, final crack pattern

### 3.3 Crack pattern for the restrained specimens

The primary cracks start at the top side of the anchor head as for the non-restrained specimens. However, their inclination is much less due to the changed direction of the principal stresses as a result of the lateral restraint. This crack pattern corresponds to the first maximum load. With increasing displacement  $v$  the primary cracks extend towards the specimen sides with a slight upward inclination. Failure occurs when the cracks reach the specimen sides, see Fig. 7. Crushed zones near the anchor head and at the upper corners of the specimen result from the action of the restraining stress. No essential differences in the crack pattern could be observed for the three materials used.

Specimen R2-1, having a shorter distance between the supports ( $a=62.5$  mm), exhibits a crack pattern consisting of primary cracks with a steeper inclination. With increasing displacement  $v$  these cracks did not reach the specimen sides but ended at the top surface.

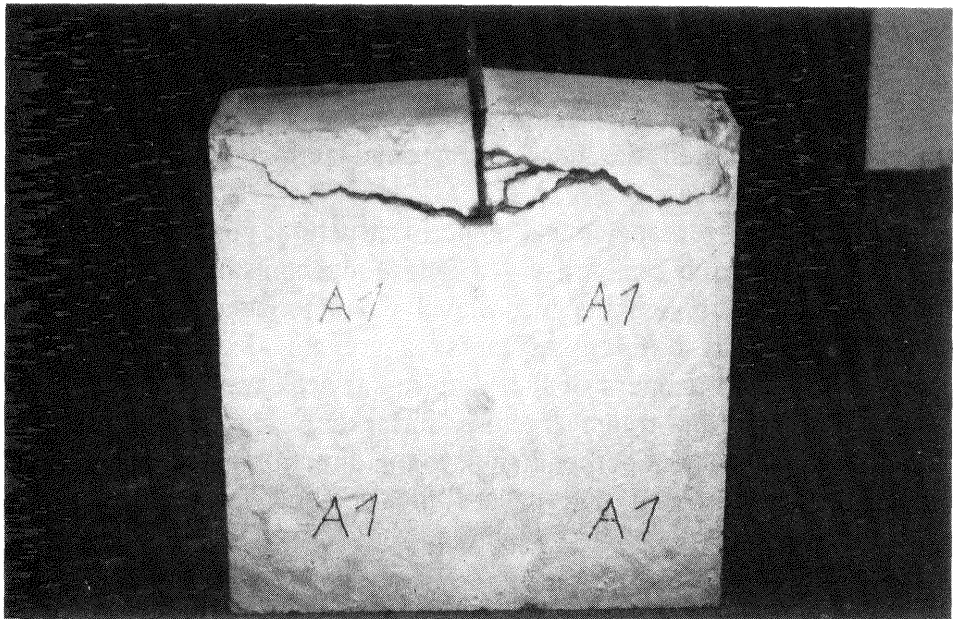


Fig. 7. Specimen R1-1, final crack pattern

## 4 Discussion of the failure process and conclusions

1. Initial cracks start to grow symmetrically from both sides of the bolt head. Their inclination is always less than what would be predicted by assuming a shear failure mode according to classical continuum

mechanics. The opening of these first cracks induces a rotation of the two separating concrete pieces on each side of the anchor bolt. This rotation and the shear induced dilatancy are partially restrained by the stiff anchor bolt and give rise to a splitting force.

2. The induced splitting force determines the final crack pattern. Origination and path of the splitting cracks depend on the boundary conditions. For a short span between the supports, a centered vertical crack develops under the bolt head. For a wide span, the initial cracks propagate with a gentler inclination than in the previous case. They develop nearly horizontal and the induced splitting force acts too close to the specimen side faces. As a consequence, instead of one single centered crack, two symmetric splitting cracks originate from the initial cracks heading downwards to the specimen side faces.
3. For the restrained specimens a different fracture behavior could be observed. The primary cracks propagate almost horizontally starting from the anchor head. This is due to the fact that the high horizontal restraining stress gives rise to a nearly vertical principal tensile stress. Due to the hindered horizontal displacement, splitting forces are no longer induced and, consequently, the continuous drop of the applied load is prevented. Under these conditions no vertical crack can develop. Final failure occurs when the nearly horizontal primary cracks reach the specimen side faces.
4. Tests were run with specimens made of structural concrete, mortar and lightweight concrete. The observed failure mechanism was the same for all materials. Although the meso-level characteristics of the materials were significantly different as far as aggregate size and strength are concerned, the roughness of the fracture surfaces was comparable. The interlocking of the rough fracture surfaces in conjunction with the hindered displacement perpendicular to the direction of the pull-out force prevents crack sliding and causes the opening mode crack pattern observed here.

## References

Alvaredo, A.M., Slowik, V., Wittmann, F.H. (1992) Experimental study on the fracture of anchorage of bolts. contribution to RILEM (1990).

RILEM TC 90-FMA (1990) Round Robin analysis and tests of anchor bolts - invitation. **Materials and Structures**, 23, 78.